Experimental and *ab initio* study of the structural and electronic properties of subnanometer thick Ag films on Pd(111)

V. Mikšić Trontl
Faculty of Electrical Engineering and Computing, Unska 3, HR-10000 Zagreb, Croatia

I. Pletikosić, M. Milun, and P. Pervan*
Institute of Physics, P.O. Box 304, HR-10000 Zagreb, Croatia

P. Lazić, D. Šokčević, and R. Brako
Institute Ruđer Bošković, P.O. Box 180, HR-10000 Zagreb, Croatia

(Received 2 September 2005; revised manuscript received 26 October 2005; published 16 December 2005)

We present a combined, experimental, and computational investigation of the growth mode and the valence-band structure of Ag/Pd(111), with the focus on the Ag 4*d* derived quantum well states. Low-energy electron diffraction and scanning-tunneling microscopy are used to determine epitaxial, layer-by-layer growth of silver on the palladium substrate. High-resolution (in both energy and angle) photoelectron spectra and *ab initio* density-functional band-structure calculations are compared for 1 and 2 ML silver films along the $\bar{\Gamma}-\bar{M}'$ high symmetry line of the surface Brillouin zone. The observed *d*-derived electronic states and their dispersion are explained in terms of quantum well states. The interaction of the silver 4*d* electronic states with the palladium substrate is discussed.

DOI: 10.1103/PhysRevB.72.235418 PACS number(s): 68.55.Jk, 68.35.Fx, 68.37.Ef, 68.65.−k

I. INTRODUCTION

Growth of metal ultrathin films on top of metallic surfaces can lead to virtually decoupled electronic systems of the film and the substrate. Partial energy gaps or just different symmetry of electrons in the overlayer with respect to those in the substrate at the same energy will lead to confinement of electrons within the film. These stationary states, known as quantum well (QW) states have been observed in a large number of metal-on-metal systems.[1,2]

The *s*-*p* derived QW states have been reported for many systems,[1,2] while study of the *d*-derived QW states is less common.[3–8] The spectroscopy of *d*-QW states is hampered by the fact that already for a few monolayer thick films there are dozens of states that are localized in a narrow energy range, i.e., the energy window limited by the overlap of the film *d*-band width with the substrate energy (or symmetry) gap. High energy resolution spectrometers are required to resolve, at most, just a few of individual QW states. One of the early detailed analyses of the electronic properties of Ag-4*d* was reported by Tobin *et al.* for the well-known (10×2) silver monolayer film on Cu(100).[9,10] A development and dispersion of the 4*d* bands in Ag(111) monolayers deposited on different metal and semiconductor surfaces were studied by Shapiro *et al.*[11] The *d*-QW states of Ag films on metallic substrates were reported for W(110),[3–5] Fe(100),[6] V(100),[7] Ta(110),[12] and Cu(100)[13,14] surfaces.

Silver and palladium both have fcc structure, with bulk lattice constants of 4.09 Å and 3.89 Å, respectively. It has been found that at room temperature silver forms on a Pd surface perfectly ordered layer without any interdifusion[15–17] at the interface, which is essential for the formation of QW states. On the other hand, palladium and silver alloy at all concentrations. X-ray appearance near-edge structure (XANES) and x-ray-photoemission study of Ag-Pd alloys have shown[18] that, due to the alloying, both constituents (Ag and Pd) gain *d*-charge and lose charge of *s* and *p* symmetry. However, it is not clear if relaxation effects have been properly taken into account. Steiner and Hufner[19] applied the $Z+1$ approximation to analyze Ag_xPd_{x-1} alloys and have found that relaxation effects on Pd components dominate the Ag 3*d*-level shifts. Previous LEED measurements have shown that silver grows on (111) surface of palladium epitaxially, layer by layer.[20] Significantly lower surface free energy of silver (111) surface ($0.62\ J/m^2$) with respect to Pd(111) ($1.22\ J/m^2$) is the main driving force for the layer by layer growth. In-plane lattice constant of silver in bulk Ag(111) is 0.289 nm which is by 5% bigger than the corresponding lattice constant of Pd. This small mismatch has an observable influence on the growth of silver layers; on one hand it is small enough for the silver to grow in registry with the palladium surface, and on other hand the photoelectron diffraction and low-energy electron diffraction (LEED) measurements have shown that silver overlayer film has fcc structure with a stacking fault between the first and second silver layers.[20] It has also been shown that the silver film structure is temperature dependent.[21] Exploring the fact that surface states reflect a growth mode of the overlayer film, the two-photon spectroscopy of the image states was used[21] to characterize the structure of the silver layers. It has been found that the silver monolayer retains a sharp interface with palladium surface up to 370 K. Above this temperature, the alloying process starts and, when the film is annealed up to 670 K, a homogeneous surface Ag-Pd alloy is formed. Annealing at temperatures above 900 K recovers clean Pd surface.[21]

In this paper we present experimental and computational investigations of the valence-band structure of Ag/Pd(111)

with the focus on the development of the Ag-4*d* bands. We use LEED and scanning-tunneling microscopy (STM) to characterize the substrate surface as well as the structure of the films. High-energy and -angle resolution photoelectron spectroscopy (ARPES) provides direct information on the energy-momentum dispersion of the electronic states in the valance band of the films. The *ab initio* calculations of the Ag/Pd(111) system were performed in the density-functional theory (DFT) approach. Comparing the experimental results to the theoretical calculations, we show that the electronic structure of the Ag-4*d* bands around the center of the surface Brillouin zone can be understood in terms of QW states (bands). We could also explain dispersion of the Ag-4*d* bands for 1 and 2 ML Ag films. Comparison to the calculation for the unsupported Ag films suggests that the 4*d* bands in 1 and 2 ML thick silver films are only weakly perturbed by the palladium substrate.

II. EXPERIMENTAL AND COMPUTATIONAL DETAILS

The experiments were carried out in an ultrahigh vacuum chamber with the base pressure in the range of 10^{-8} Pa. The chamber was equipped with STM[22] and rear-view LEED. For the photoemission experiments we used a Scienta SES-100 hemispherical analyzer which simultaneously collects photoelectrons at a range of energies (in this experiment typically around 5 eV) and angles (around 12°) and a discharge lamp as an excitation source. The ultimate instrumental resolution of the analyzer is around 5 meV, whereas in this experiment the estimated energy resolution was around 25 meV. The binding energies could be read from the photoemission spectrum with an uncertainty of ±0.01 eV. The angular resolution was around 0.2°. The He I (21.2 eV) and Ne I (16.8 eV) photons were used for excitation in photoemission spectroscopy experiments. The polar angle was changed by rotation of the sample along $\Gamma-\bar{M}'$ (positive polar angles) and partly along the $\Gamma-\bar{M}$ surface symmetry line (negative polar angles). The $\bar{M}'$ edge is reached by 21.2 eV (16.8 eV) excitation energy at a polar angle of 45° (55°), respectively. The experiments were performed using two sample holders. The one for the photoemission experiments allowed cooling and heating of the sample in the temperature range between 150 K (obtained by a Leybold He cold head) and 1200 K (obtained by resistive, direct heating by thin tantalum wires). All photoemission spectra shown in this work were taken at 150 K substrate temperature. The sample holder specially designed for the STM measurements did not allow cooling, only heating (up to 1200 K), and therefore all STM measurements were performed at room temperature. Palladium crystal of nominal purity of 99.99% was oriented with the precision of 0.1° and mechanically polished. Further cleaning of the crystal was performed in the UHV chamber. We used palladium single step height to additionally calibrate STM vertical resolution in this experiment. The step height was set to be 0.23 nm. Silver films were prepared by resistive heating of a tungsten basket filled with pure silver. The deposition rate was adjusted to be 0.2–1 ML/min.

The *ab initio* calculations were performed in the density-functional theory (DFT) approach, using the DACAPO computer code. We used periodic boundary conditions in all three spatial directions, modeling the Pd substrate by six hexagonal layers and a vacuum region of sufficient thickness, which separates the periodically repeating Pd slabs. The details of the method are described elsewhere.[23] The lattice constant of Pd was taken to be 0.399 nm, which is the equilibrium value for our calculations of bulk Pd, and differs slightly from the experimental value of 0.389 nm. This choice is necessary in order to avoid the appearance of spurious stress in the modeled substrate. The bottom three Pd layers were kept fixed at bulk separation, and the top three layers of the substrate and silver layers were allowed to relax freely in the direction perpendicular to surface (z coordinate).

In calculating the electronic bands of ultrathin silver films we have found the silver *d* states appearing about 1 eV too close to the Fermi level when compared to the peaks observed in the photoemission experiments. This deficiency of the Kohn-Sham eigenstates of *d* orbitals obtained in density-functional calculations of silver and other noble metals has been known for some time.[24] Furthermore, the calculated silver 4*d* bands are spin degenerated because the calculations do not include the spin-orbit coupling.

III. EXPERIMENTAL RESULTS

A. Clean palladium surface

The substrate Pd(111) surface was prepared by cycles of Ar^+ sputtering followed by a flash to 1200 K and prolonged annealing at 1000 K in the oxygen atmosphere (partial pressure of oxygen was kept at 1×10^{-5} Pa). The clean and annealed Pd(111) exhibits a sharp (1×1) symmetry LEED pattern while STM measurements show 50–150 nm broad palladium terraces. Figure 1 shows the photoemission of the clean and well-annealed Pd(111) as a function of energy and electron emission angle in the form of an intensity gray-scale map. For every 5°, a cut along the binding energy axis [corresponding to an energy distribution curve (EDC)] is shown as well. The obtained EDCs are qualitatively identical to the spectra obtained by Kang *et al.*,[25] except that photoemission peaks are narrower. This might be due to the combined effect of a better analyzer resolution and lower substrate temperature. Namely, for the normal emission (NE), the width and the height of the peak at 1 eV binding energy (BE) shows rather strong dependence on the substrate temperature, indicating that the electrons in the corresponding band couple to the phonon excitations.

It is not a surprise that the palladium surface could stay clean in the existing experimental condition for a longer time without being significantly affected by the residual gas adsorption.[26] Even if the surface was slightly contaminated by the adsorption from the residual gas the effects could not be seen in the NE spectra. The effect of slight carbon monoxide or hydrogen adsorption (main constituents of the residual gas in our chamber) could have been observed mainly in the off-normal spectra, close to the $\bar{M}'$ edge of the surface Brillouin zone. If the sample is left for about 30 min at

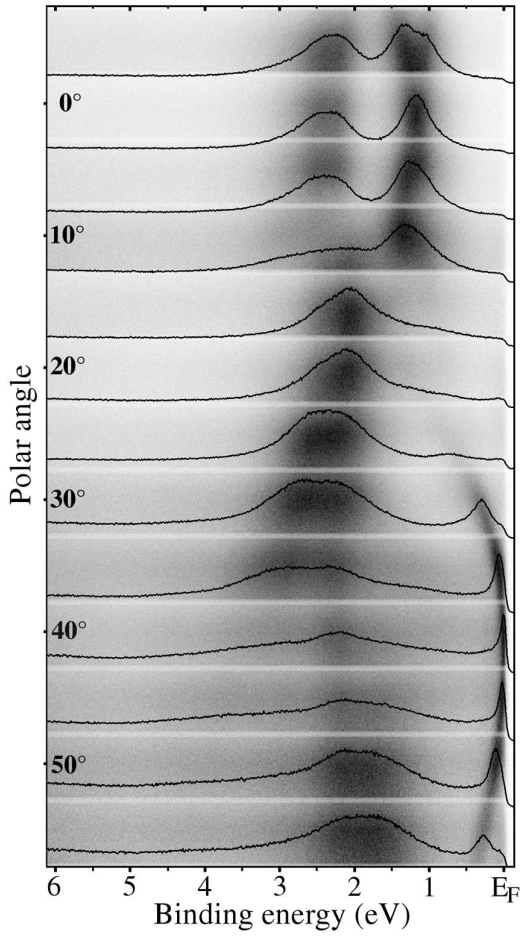

FIG. 1. Photoemission intensity gray-scale map of Pd(111) along $\bar{\Gamma}-\bar{M}'$ high symmetry line. For each 5° of the polar angle, a corresponding energy distribution curve (EDC) is shown as well. Photon energy: He I line at 21.2 eV.

150 K, a new peak develops at binding energy (E_B) equal to 0.3 eV. At the same time there is a significant intensity reduction of the peaks at the Fermi level and E_B=3.2 eV (Fig. 2).

B. Ultrathin Ag films

1. LEED and STM

The films were deposited on the clean and annealed palladium surface at room temperature. For all film thicknesses studied, our LEED measurements have shown a pseudomorphic growth of the silver overlayer.

Figure 3 shows a set of STM images of Pd(111) surface covered with different amounts of silver (corresponding coverage and the parameters of the STM are given in the figure caption). A STM image of a clean and well-annealed Pd(111) surface is shown in Fig. 3(a). The growth of Ag on Pd(111) starts with the decoration of palladium step edges [see Fig. 3(b)] and continues with the growth of islands without a preferential growth direction; although, some films appear to be elongated across the terraces. In addition, a number of small islands of a typical size 3–5 nm are dispersed over

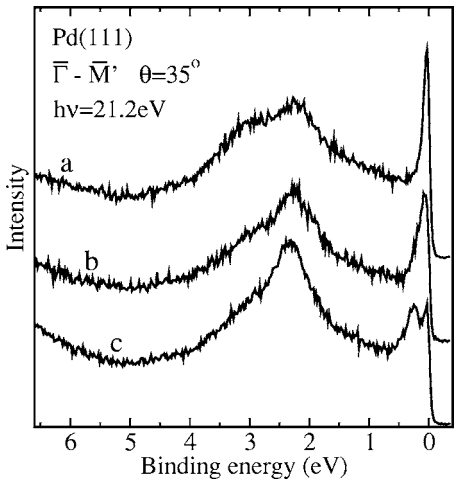

FIG. 2. Photoemission spectra of Pd(111) taken at a 35° polar angle (a) immediately after the cleaning procedure, (b) 15 min later, and (c) 30 min later.

palladium terraces [Fig. 3(b)]. These islands are not stable at room temperature, and in the course of time (typically few hours), they migrate across the terrace and eventually merge with bigger ones. A similar pattern was observed for the 0.5 coverage with the only difference that the average size of the islands increased (the corresponding STM image is not shown).

At the coverage of 0.75 ML most of the silver islands have reached the width of the palladium terraces and further growth goes as a widening of the islands along the terraces [see Fig. 3(c)]. At the nominal saturation coverage (1 ML) most of the surface is covered with silver with the characteristic fuzzy step edges [see Fig. 3(d)]. Only when the first layer is completely saturated does the growth in the second layer start [see Fig. 3(e)] again from the step edges. This stage is characterized by a relatively large number of small unfilled areas that run along the steps that are indicated by arrows in Fig. 3(e).

Although the growth pattern in the second layer is virtually the same as in the first layer, there is one distinct difference. Namely, as Fig. 3(f) shows, when an island in the second layer reaches the width of the terrace it continues to grow across it, extending to the lower terrace where it presents the third layer. In this manner, growth of the third layer starts before the second layer is completely saturated, indicated by number of layers in Fig. 3(g). The further growth of silver film is characterized by clear layer-by-layer growth mode and overall increase of the terrace width. Figure 3(h) shows that only occasionally can isolated islands form on top of a flat silver terrace. From a number of independent STM measurements on different parts of the surface, we have concluded that the step height of the single monolayer silver film is 0.25±0.02 nm, independent of the island size. The step height of the second silver layer, with respect to the first one, is 0.23±0.02 nm.

2. Photoemission

Figure 4 shows normal emission (NE) spectra of different coverages of Ag on Pd(111) taken with He I (21.2 eV) pho-

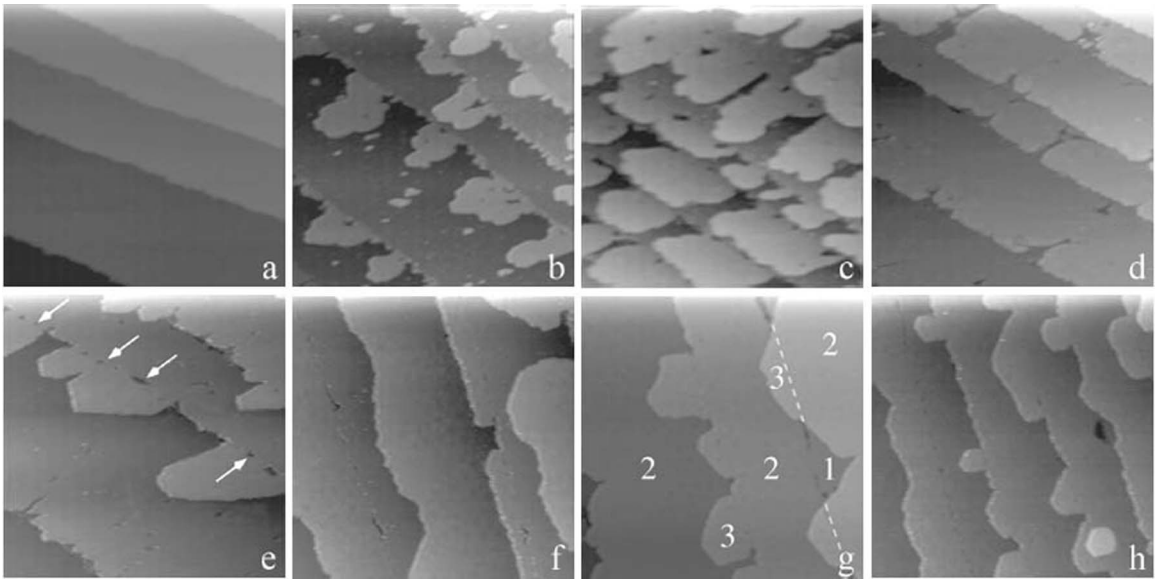

FIG. 3. STM images of Pd(111) covered with different amounts of silver. All images represent area of 116×116 nm^2, obtained using bias voltage $U=0.5$ V and tunneling current I=0.2 nA. Images correspond to (a) clean Pd(111), (b) 0.25 ML Ag, (c) 0.75 ML Ag, (d) 1 ML Ag, (e) 1.25 ML Ag, (f) 1.5 ML Ag, (g) 2 ML Ag, and (h) 3 ML Ag.

ton excitation energy. The NE spectra of a submonolayer and monolayer Ag films are characterized by two peaks, at 4.21 and 4.48 eV, referred to as *a* and *b*, respectively [see Fig. 4(a)]. Figure 4(b) shows that the BE of both peaks is independent of the silver coverage in the whole submolayer range. A further increase of the silver coverage and growth of the second layer induces several effects in the photoemission spectrum [Fig. 4(a)]. There is a clear reduction of the height of peaks *a* and *b* and their slight shift to 4.18 and 4.45 eV, respectively. In the second layer we refer to these states as to *e* and *f*. In addition, a new set of peaks (*g*–*j*) appear at 4.61, 4.84, 5.45, and 6.0 eV. With increasing Ag coverage, the intensity of the palladium peaks decreases. Note, however, the peak closer to the Fermi level is reduced more efficiently. Despite the high-energy resolution of the analyzer, with a further increase of the silver film thickness it is not possible to distinguish individual states.

The photoemission spectra of multilayer silver films are dominated by the spectral maximum at 4.84 eV. Also, there is a shift of peaks *i* and *j* to 5.65 and 6.10 eV, respectively. For the coverage equivalent to 7 ML, there are four states associated with the silver 4*d* bands that could be observed with 21.2 eV photon energy; the most prominent peak at 4.89 eV with the shoulder at low BE side (4.30 eV) and two peaks of the same intensity at 5.65 and 6.10 eV. At this coverage, the palladium valence-band peaks could not be seen in the spectrum. The peak at the Fermi level is a silver surface state, whereas the peak at 3.04 eV is probably a satellite induced by the 23.1 eV excitation energy.[27,28]

Figure 5 shows photoemission intensity maps of the valence bands of Ag/Pd(111) at 1 and 2 ML Ag coverage, for different polar angles, taken with He I and Ne I excitation energy. By using two excitation energies one may, on the one hand, distinguish between bulklike states (they disperse with changing photon energy) and two-dimensional [(2D), e.g., surface] states (they do not disperse with changing photon energy), and on the other hand, gain some benefit from different excitation cross sections of electronic states at different excitation energies. However, one should bear in mind that the Ne I line is, in fact, a doublet (split by 18 meV), which leads to some broadening when compared to the He I spectra.

The most prominent features of the 1 ML intensity plot around the center of the surface Brillouin zone ($\Theta=0°$) are silver states *a* and *b*, which disperse negatively [see Fig. 5(a)]. State *a* disperses through the whole range of polar angles, from 4.21 eV at $\Theta=0°$ to 4.65 eV for $\Theta=45°$ ($\Theta=55°$ for Ne I).

The spectral intensity of state *b* decays rapidly between $\Theta=10°$ to $\Theta=15°$. Another prominent feature of this 2D plot is positively dispersing state *c*, which in the case of 21.2 eV photon energy, starts to be clearly visible at $\Theta=20°$ as a high-energy shoulder of the peak corresponding to band *a* and as a low-energy shoulder of the same state at $\Theta=25°$. Although the spectral intensity is rather weak, state *c* can be traced down to $\Theta=5°$, where the BE is estimated to be 5.20 eV. For He I excitation this silver band reaches the minimum BE (3.50 eV) at the polar angle of $\Theta=45°$. The band labeled *d* shows slight positive dispersion starting from $\Theta=30°$, where the corresponding photoemission maximum can be identified at 5.20 ± 0.03 eV. With increasing polar angle, the peak associated with this band gains on the intensity and shifts to lower binding energies and at the edge of the Brillouin zone reaches 5.0 eV. This band is better resolved with 16.8 eV photon energy [Fig. 5(c)].

The 2 ML spectra are shown in Figs. 5(b) and 5(d). The electron bands are indicated by letters *e*–*m*, consistent with the annotation in Fig. 4(a). The Ne I spectra in Fig. 5(d) show only a fraction of the bands that can be observed with He I. The set of bands *e*, *f*, *l*, *k*, and *m* is qualitatively very similar to the set of bands *a*, *b*, *c*, and *d* associated with the 1 ML film [see Fig. 5(a)]. In the center of the Brillouin zone,

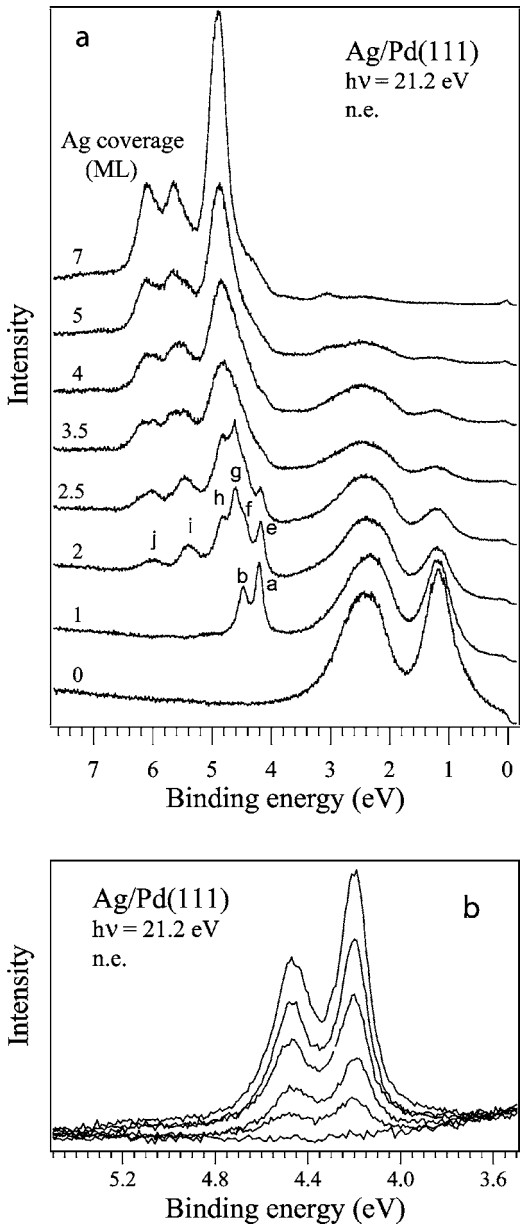

FIG. 4. (a) NE spectra of Pd(111) covered with silver films of different thickness (film thicknesses are indicated in the figure). The peaks associated with electron states in 1 and 2 ML films are indicated by letters (a–k) in accordance with the spectra shown in Fig. 5(b). (b) Same as (a) but only for submonolayer silver coverages: 0, 0.15, 0.30, 0.50, 0.70, and 1.0 ML.

bands e and f are shifted with respect to bands a and b to lower BE by only a few millielectron volts. On the other hand, at the edge of the zone, band k is at 3.35 eV, which is by 0.10 eV a lower value than band c has at the same point of the zone (3.45 eV). At first glance it looks as if bands e, f, and k disperse in the very same fashion as bands a, b, and c, respectively. From the He I spectra it is not clear if band l crosses bands e and f or if it folds back around $\Theta = 25°$ and disperses as band e. However, from Fig. 5(d), it is clear that band e in the first part of the Brilloun zone disperses negatively and than changes the character and disperses positively as band l. Band j around at 6.05 eV in NE is flat up to $\Theta = 30°$ [see Fig. 5(c)], whereas at higher energies it disperses away from the Fermi level to 6.25 eV.

IV. CALCULATION OF STRUCTURAL AND ELECTRONIC PROPERTIES OF Ag/Pd(111)

A. Structure of silver layers

This and previous experimental investigations have found that silver films grow in registry on the Pd(111) substrate. Since previous experimental results indicated that a stacking fault takes place between the first and the second silver layer, resulting in a twinned crystalline structure,[20] we have calculated various configurations of Ag layers on a Pd substrate, both with and without a stacking fault.

First, we have taken the fcc palladium (in our calculation this is six hexagonal layers of atoms stacked in the fcc ABCABC order) and added one to three layers of Ag continuing the regular fcc ordering (e.g. ABCABC—AB), allowing the relaxation. Next, we have calculated the structures in which a silver layer (in particular, the second one) goes into the hcp position, resulting in structures like ABCABC—AC, etc.

The calculated interlayer distances and adsorption energies are shown in Table I. The adsorption energy per atom is around 2.84 eV for Ag atoms in the first layer, decreasing to around 2.50 eV for Ag atoms in the second layer, and to 2.52 eV in the third layer. The energy is virtually the same for the second layer adsorbed in "regular" fcc sites (AB) and in the "wrong" hcp sites (AC), i.e., with a stacking fault. The slight preference of 0.4 meV for the regular structure is, in fact, smaller than the expected accuracy of the DFT calculation.

In order to investigate the energetics of the initial nucleation of the second silver layer, we have calculated configurations in which, on top of a fcc Pd-Ag structure, there is an extra silver atom at a 1/4 coverage, either in the fcc or in the hcp threefold hollow site. We used a 2×2 supercell along the surface plane, with three sites in the last layer empty and one occupied. We found that the adsorption energy is around 1.90 eV, which is about 0.6 eV less than the energy per atom in the full silver monolayer. The adsorption of the Ag atom is marginally favorable by 0.6 meV if it sits in the hcp instead of the fcc site, but the difference is too small for an unambiguous interpretation. This difference is still too small to be considered relevant for the growth mode, especially as the STM images show that the third layer starts growing from steps and not by nucleation on terraces.

We have also calculated the energies of 1–3 ML Ag films with some other stacking orders, but those appear to have less favorable energies. In particular, the structure where a monolayer of Ag is already in hcp sites has an energy value larger than that of the fcc Ag monolayer by around 8 meV, effectively ruling out this mode of growth.

B. Electronic bands

In order to understand the electronic structure of ultrathin silver films on Pd(111), we have first made calculations of both the electronic bands of the palladium bulk and of unsupported silver films.

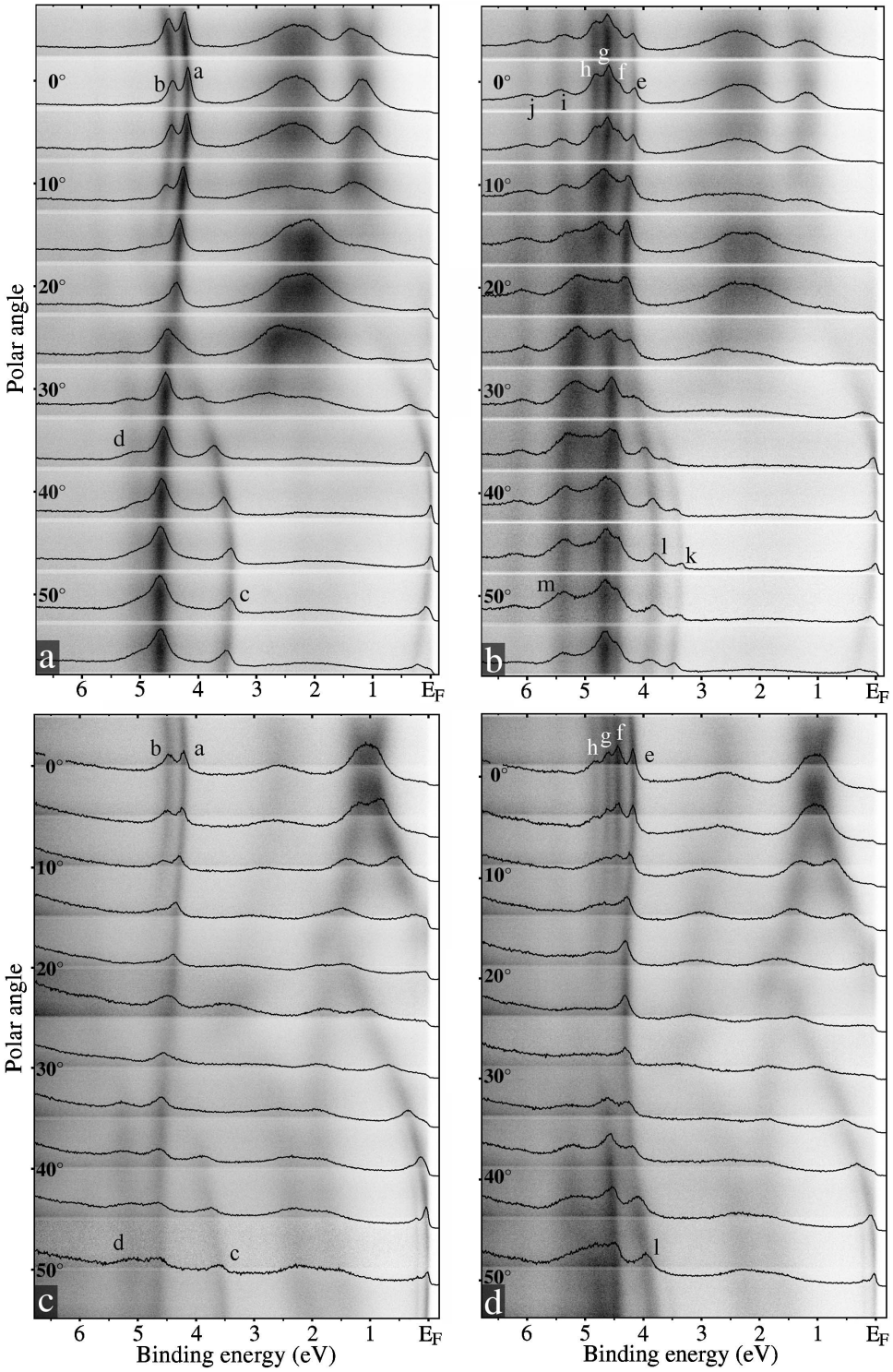

FIG. 5. Photoemission intensity gray-scale map of 1 ML (a,c) and 2 ML (b,d) of Ag on Pd(111) measured along $\bar{\Gamma}-\bar{M}'$ high symmetry line. The spectra are taken with He I (21.2 eV) (a,b) and Ne I (16.8 eV) (c,d) excitation energy. For each 5° of the polar angle, a corresponding energy distribution curve (EDC) is shown as well.

1. Projection of bulk Pd states onto the Pd(111)

In Fig. 6, we show the calculated electronic structure of bulk palladium along the (111) direction [see Fig. 6(a)] and the band structure projected onto the surface Brillouin zone (SBZ) for the (111) surface in the $\bar{\Gamma}-\bar{M}$ and $\bar{\Gamma}-\mathrm{K}$ directions, for around 30 values of k_{111} [Fig. 6(b)]. We should point out that in this picture the directions $\bar{\Gamma}-\bar{M}$ and $\bar{\Gamma}-\bar{M}'$ are equivalent.

At the $\bar{\Gamma}$ point of the SBZ, the *d* bands occur from just below the Fermi level to 3 eV, and there is an energy gap in the projected states from around 3 eV to just above 5 eV below the Fermi level. The gap becomes smaller at finite $k_{\|}$ and closes around the half of the surface Brillouin zone.

2. Unsupported silver films

Figure 7 shows the results of our calculation for the electronic structure of unsupported two-dimensional hexagonal

TABLE I. Calculated step heights, interlayer distances (all in nanometers), and adsorption energies per atom for Ag layers on Pd(111). For two and more Ag layers, both the regular fcc structure and the structure with a stacking fault between the first and second layers (Ag_1 and Ag_2) have been calculated. The Pd substrate is modeled by six hexagonal layers with nearest-neighbor interatomic distances of 0.282 nm. The clean Pd surface shows no appreciable relaxation, i.e., all distances between Pd layers are 0.230 nm.

	1 ML Ag	2 ML Ag	2 ML Ag with stacking fault	3 ML Ag	3 ML Ag with stacking fault	4 ML Ag	4 ML Ag with stacking fault
Step height	0.237	0.234	0.244	0.242	0.232	0.246	0.246
Ag_3-Ag_4						0.244	0.243
Ag_2-Ag_3				0.244	0.244	0.242	0.242
Ag_1-Ag_2		0.242	0.245	0.241	0.241	0.242	0.242
Pd_1-Ag_1	0.236	0.234	0.236	0.233	0.233	0.234	0.235
Pd_1-Pd_2	0.231	0.229	0.232	0.229	0.229	0.230	0.230
Pd_2-Pd_3	0.231	0.228	0.231	0.229	0.229	0.229	0.229
Pd_3-Pd_4	0.230	0.228	0.229	0.228	0.228	0.230	0.229
Pd_4-Pd_5, etc	0.230	0.230	0.230	0.230	0.230	0.230	0.230
Adsorption energy (eV)	2.844	2.500	2.500	2.528	2.521	2.511	2.511

lattice of Ag atoms (i.e., one or two layers of Ag atoms with vacuum on both sides). The interatomic distance of Ag atoms was set to 0.23 nm, corresponding to the interatomic separation of Pd(111), along the high symmetry directions of the BZ. In the case of single silver layer (full curves) narrow *d* bands are located between 2.8 and 5.0 eV BE (at $\bar{M}$ point), while the broad *sp* band starts from 6.3 eV and crosses the Fermi level near the outer edge of the two-dimensional BZ, hybridizing strongly with the *d* bands while crossing their energy range. The symmetry of the states at the $\bar{\Gamma}$ point indicated in the figure was determined from the projection of the calculated bands onto atomic orbitals, the *z*-axis being perpendicular to the surface. Of course, away from the $\bar{\Gamma}$ point only the broad separation into *sp* bands, easily recognized by strong free electronlike dispersion, and narrow *d* bands remains valid, and the symmetries within the *d*-band manifold are not well defined.

Here we again mention that in our calculations of the band structure of Ag films on various substrates the Kohn-Sham *d* bands appear about 1 eV too close to the Fermi level when compared to peaks observed in photoemission. This is a known deficiency of the density-functional eigenstates of silver and other noble metals,[24] and we presume that is also present in all calculations in this paper. Furthermore, our calculations do not include spin-orbit splitting of silver *d*-bands, which is easily observable in experiments.

The electronic structure of a similar two-layer hexagonal structure, with such interlayer spacing that all distances between the neighboring silver atoms are around 0.23 nm, is shown in Fig. 7 (dashed line). The bands look similar to the single-layer structure, but their number increases. The similarity is particularly evident around the $\bar{\Gamma}$ point, where the main effect is just the doubling of the number of bands.

3. 1 and 2 ML Ag on Pd(111)

In Fig. 8 we show the band structure of a monolayer and two layers of Ag atoms adsorbed on a Pd(111) surface. The thickness of the lines indicates the degree of localization of the states on the adlayers, emphasizing the silver-induced and interface states, which are most likely to be clearly visible in photoemission spectra.

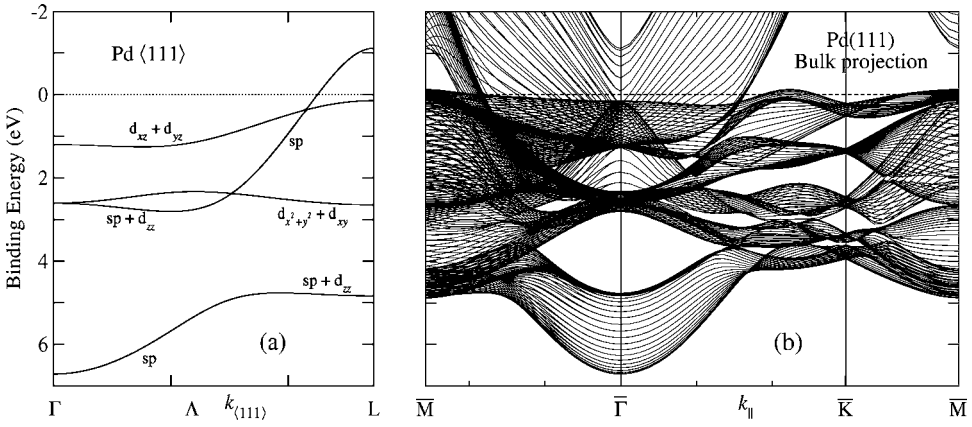

FIG. 6. (a) Calculated electron structure of bulk palladium: (a) Along k_{111} direction and (b) projected onto (111) surface Brillouin zone, for several values of k_{111}.

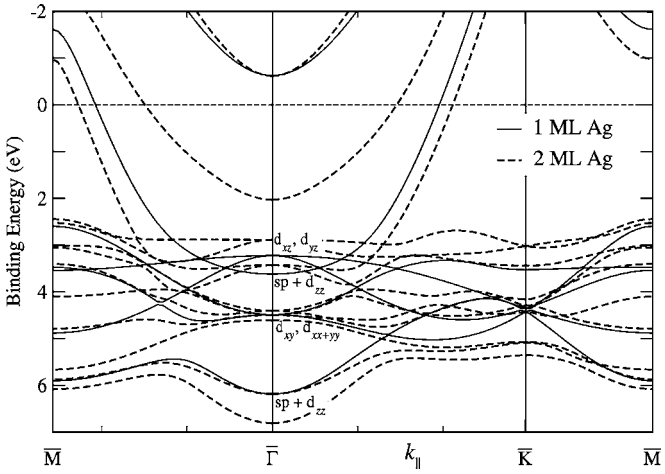

FIG. 7. Electronic eigenstates of unsupported single (solid line) and double (dashed line) hexagonal layer of Ag atoms, along the high-symmetry directions in the two-dimensional Brillouin zone. The symmetry of 1 ML states at the $\bar{\Gamma}$ point is indicated.

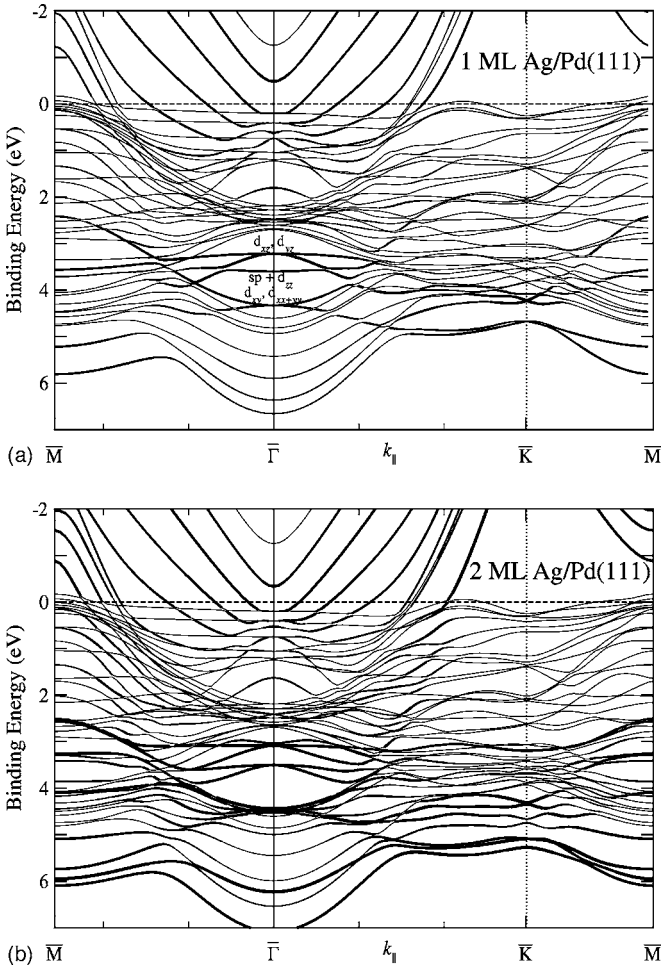

FIG. 8. Electronic eigenstates of a (a) single and (b) double layer of Ag atoms adsorbed on a Pd(111) surface, along the high-symmetry directions in the surface Brillouin zone. The thickness of the lines shows the degree of localization of the states near the surface.

Comparing the energies of *d* bands in unsupported and supported silver monolayer, we observe that the palladium substrate has induced virtually no energy shifts in the center of the SBZ. Only d_{xy}, d_{xx+yy} bands are pulled to slightly higher binding energies. A rather weak influence of palladium on the energies of *d* bands is present for two monolayer film, as well. There is only a slight shift to higher binding energies of the topmost d_{xz}, d_{yz} band. For both film thicknesses, the main features of the unsupported *d* bands away from the center of the SBZ, along $\bar{\Gamma}-\bar{M}$, are generally preserved. However, our calculation may underestimate the influence of the Pd substrate on the silver *d* bands. Namely, because of the mentioned discrepancy of the binding energy, which is too small by about 1 eV, a too-large portion of the calculated bands lies in the energy gap of Pd at and around the $\bar{\Gamma}$ point and is therefore completely decoupled from the substrate bands, whereas, in reality, they exit the gap much sooner.

A recent work[7] presented a discussion of the *d*-QW states of Ag on V(100) in the light of the tight-binding calculations presented in the paper and in several previous theoretical studies. In that system, the *d*-QW states appear particularly clearly in photoemission spectra because of the favorable gap of states of the corresponding symmetry in the band structure of V(100).

V. DISCUSSION

A. Structure and growth

Despite the 4.8% difference in the size of the silver and palladium unit cells, silver grows in registry with the palladium crystal lattice. A rather big difference in the adsorption energies for a silver atom on palladium and silver monolayer surfaces (2.84 and 2.50 eV, respectively) indicates good wetting of the palladium surface by silver overlayer. Indeed, as STM measurements have shown, silver initially grows by preferential adsorption on palladium. Only when the first silver layer is completely saturated does the growth of the second layer sets in.

A general pattern associated with the growth of the first silver layer on Pd(111) is a dominance of large islands that grow from the step edges and relatively small number of scattered islands, which, in the course of time, migrate over the surface and merge with the big islands. The growth of the second and the third silver layer is almost exclusively realized through the enlargement of small number of islands following the layer-by-layer mode. Since the silver adatom acquires a substantial amount of energy adsorbing at the edge of a silver island with respect to adsorption of an isolated atom, the islands will expand irrespective of the number of underlying silver layers. The consequence of such growth is, as Fig. 9 suggests, that third silver layer will start to grow before the second one is completed. Our calculations show that the adsorption energy of third silver layer (2.53 eV) is bigger than for the second one (2.50 eV).

Our experimental results do not provide any further arguments if a stacking fault takes place between the first and the second silver layers as it has been reported by Eisenhut *et*

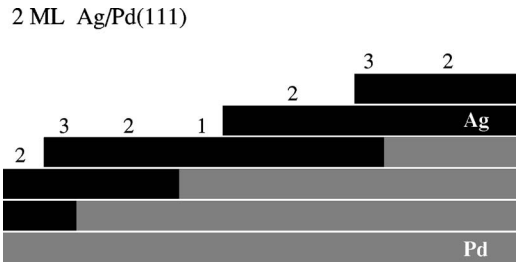

FIG. 9. Structural model of Ag/Pd(111) for the nominal coverage of 2 ML. Schematics indicates the growth of the third silver layer before the second one is saturated.

al.[20] Our calculations, however, indicate that the energy balance does not prefer fcc stacking with respect to hcp. Analogous formation of a stacking fault between the first and the second adlayer has been observed during Ag growth on Pt(111) at room temperature, but the second layer reverts to the fcc sites after annealing to 750 K.[29] In that system, further Ag layers continue to grow in fcc stacking order with respect to the first two Ag layers, i.e., with or without a stacking fault depending on whether the second layer was annealed. The stacking order of thicker Ag films on Pt(111) is not changed by annealing.[29] We must stress that the energy difference between various configurations obtained in *ab initio* calculations of Ag on Pd(111) are very small and cannot be regarded as a definite explanation of the growth mode. It has been suggested that the occurrence of a stacking fault between the first and second silver layers in the case of Ag growth on Pt(111) is a consequence of the kinetics of the adlayer growth rather than of a more favorable energy.[29] When discussing the energy preference of the stacking orders of silver atoms on Pd(111) one should bear in mind that the present theoretical results are obtained assuming the adsorption of silver atoms on a flat surface. However, we know from our experiments that the initial growth of each silver layer is localized to the step edges. Thus, the second layer starts appearing when the first layer on the upper step is completed and extends over the silver monolayer on the lower step. For the moment, both our experimental and theoretical results are insufficient to determine whether the transition over the step edge is regular or contains a stacking fault. If the latter is true and the growth continues until the layer is completed, the stacking fault (AC order of Ag layers) is frozen since there is no simple kinetic path that converts the whole layer into the fcc structure (AB). The third Ag layer then grows in fcc sites with respect to the first and second layers, which results in a ACB layer structure.

B. Electronic bands and photoemission

The electronic structure of ultrathin films is closely related to their thickness to that extent that it can be used to estimate the number of layers of the overlayer film, provided that the film has an ideal layer-by-layer growth. Fischer *et al.*[30] used two-photon spectroscopy to follow the growth of Ag on Pd(111) by observing distinct image states associated with different silver film thicknesses. In the same way as QW states,[31] these image states were used as a fingerprint of the completion of a particular layer. However, with the increase of the film thickness, the difference between the states becomes too small and the correlation between the image states (their energy) and particular film thickness becomes increasingly unreliable. On the other hand, in some cases as, e.g., Ag/Fe(100), the *s-p* QW states show distinctively different patterns for films of different thicknesses even when the films are as thick as 100 ML.[31] In some cases, QW states of *d* symmetry can be also used as a fingerprint of the film thickness.[7] However, the number of *d*-derived QW states increases with the film thickness in a such a way that, already for a film several monolayers thick, it is very difficult to resolve individual QW states and correlate their energy to the film thickness. Photoemission spectra of Ag/Pd(111) is a clear example of such behavior.

The symmetry of palladium states in $\bar{\Gamma}$ within the energy range of 3 eV below the Fermi level [see Fig. 6(a)] is such that silver *s-p* band can couple to the substrate states, and therefore no QW states can be formed.[32] Indeed, photoemission spectra do not show characteristic peaks associated with QW states in this energy range. On the other hand, the energy gap between 2.8 and 4.8 eV around the center of the Pd surface Brillouin zone partly coincides with the energy position of the silver 4*d* bands. In addition, below the energy gap, only states of σ symmetry (*s-p* and d_{zz}) exist. All this contributes to the confinement of *d*-electrons in the silver overlayer so that the electrons in this energy range will be well localized within the silver film acquiring the character of quantum well (QW) states.

The silver monolayer on Pd(111) is characterized by two peaks in the normal emission spectrum that we attribute to the *d*-derived QW states [see Figs. 4(a) and 4(b)]. The two-peak structure in He I NE photoemission spectra of silver monolayer has been observed on different metallic surfaces.[4] The discrepancy between the number of observed photoemission peaks and expected and calculated *d*-derived QW states can be explained by the influence of the photon energy on the excitation cross section and the dipole selection rules effective for the NE geometry.[33] The photoemission peaks at 4.21 and 4.48 eV are attributed to the spin orbit split d_{xz}, d_{yz} bands. The calculated energy of this band is, as already pointed out, at a binding energy too small by 1 eV [see Figs. 7(a) and 8(a)]. The state with d_{zz} symmetry, which is mixed with the *s-p* states (the only symmetry besides d_{xz}, d_{yz} that can be accessed by photoemission in the NE geometry[33]), is not observed in the spectrum. However, the off-normal spectra [Fig. 5(a)] suggest that the band *c*, which is clearly visible only in the second part of the Brillouin zone, closer to the $\bar{M}'$ point, disperses from the surface Brillouin center where the corresponding photoemission intensity can be seen only as a very broad high energy shoulder of peak *b*. It is possible that the emission from the d_{zz} state is responsible for this shoulder. The calculation points to this direction. As can be seen in Fig. 8(a), the band d_{zz} is further away from the Fermi level than the d_{xz}, d_{yz} bands. The only point of discrepancy between the calculation and the experiment is the corresponding BE of the state. If the calculated bands are shifted by 1 eV to higher binding energies, to account for the deficiency of the DFT formalism for the *d* orbitals, the energy of *sp*, d_{zz}

band, in the center of the SBZ, is 4.6 eV, whereas the estimated position of the d_{zz} band in experimental spectrum is 5.2 eV. As already said, the fact that DFT calculation puts Ag bands too low in BE could affect the coupling effects between silver *sp*, d_{zz} band, and palladium *s-p* band. The hybridization with the substrate states could affect the BE of the silver band and, on the other hand, substantially increase the photoemission peak width. However, we have no direct arguments that such a shift could have been induced by the coupling with the substrate.

The spin-orbit doublet d_{xz}, d_{yz} is present in NE spectra taken for all silver submonbolayer coverages deposited on Pd(111). As corroborated by STM measurements, the growth of the second silver layer corresponds to the intensity reduction of these peaks and the appearance of new structure at high binding energies. It might be surprising that the increase of the silver film thickness from first to second layer is not followed with a clear shift of the leading peaks to lower binding energies [see Fig. 4(a)], as expected for the positively dispersing bands and observed in other systems.[7,8] The calculation for 2 ML film [see Figs. 8(a) and 8(b)] shows that the new topmost bands in $\bar{\Gamma}$ are shifted only slightly to lower binding energies with the respect to the spin-orbit doublet d_{xz}, d_{yz} in the first layer. For 3 ML film, the photoemission spectrum [see Fig. 4(a)] is dominated by the peak at 4.84 eV, which, with the increasing silver film thickness, constantly gains on intensity. The energy of this peak corresponds to the energy of the direct transition peak from bulk Ag(111) surface for the 21.2 eV excitation energy.[34] The same development of the photoemission spectrum has been observed for ultrathin silver on Cu(100)[14] and Ni(111).[35] This large increase of the QW states photoemission intensity at BE, which corresponds to the bulk transition, is consistent with some previous observations.[36,37] The overlayer films have a hexagonal Ag(111) structure, and the corresponding 4*d* bands are rather flat, in particular, around the center of the Brillouin zone. Therefore, the slightly different phase conditions that the localized electronic states have to satisfy in the films of different thickness will have only a small influence on their energy. With the increase of the film thickness, there will be more and more QW states with different wavelength, but very similar binding energies that correspond to the direct transition in the photoemission spectrum of the bulk sample. Therefore, it is not a surprise that photoemission spectrum of the 4*d* bands of (111) overlayer silver films develops very quickly toward the bulk line shape. Generally, this is not the case with the states of *sp* symmetry whose energy has a strong dependence on the wave vector. A small difference in the wavelength due to the different phase conditions on the interface and the vacuum side will strongly affect energy of the state [see examples of *d* and *sp* symmetry states in Ag on Fe(100),[38,6] W(110),[3,1] and V(100)[39,7]].

The dispersion of the silver 4*d* bands along $\bar{\Gamma}-\bar{M}'$ of the SBZ is rather well described by the model calculation shown in Figs. 7 and 8. However, one should bear in mind that the calculation artificially shifts silver 4*d* bands by 1 eV too close to the Fermi level, and therefore the real effects of hybridization might be somewhat different with respect to the obtained calculation. Still, when comparing dispersion of calculated energy bands [see Fig. 8(a)] and the photoemission 2D intensity plots for one silver monolayer [see Figs. 5(a) and 5(b)], we could see a rather good qualitative and quantitative agreement. As predicted by the calculation we see the dispersion of band *a* across the whole $\bar{\Gamma}-\bar{M}'$ symmetry line and a large part of the band *c*. Apart from the energy offset of 0.5 eV, the silver bands disperse in a same fashion as on Cu(100).[9,40] The contribution from band *d* [see Fig. 5(a)] is only fractionally present in the calculated intensities [see Fig. 8(a)] compared to the measured spectra. This can be, as mentioned, an effect of artificial shift of the 4*d* bands to lower binding energies.

When compared to the calculated electronic structure of the unsupported silver monolayer we can see that most of the experimental results could have been explained in terms of unsupported silver film, indicating relatively small interaction of the silver with the underlying palladium electronic system.

The width of the photoemission peaks of QW states has been used to estimate the efficiency of the interface barrier in the confinement of the electrons in the overlayer film.[41,6] Assuming that transmission through the interface barrier is a dominant channel of photo-hole decay, one can correlate the photoemission peak width with the localization efficiency of the barrier.[6]

We have compared the width of the photoemission peaks associated with the d_{xz}, d_{yz} doublet for the monolayer film on Pd(111), this work, Fig. 4(b), and V(100).[7] The spectra were fitted with the Lorentzian function and the corresponding values of peaks *a* and *b* in Ag/Pd(111) were found to be 140 and 240 meV, respectively.

A separate set of measurements performed at 80 K gives peak widths of 120 and 180 meV, respectively, indicating the interaction of the photo hole created in the d_{xz}, d_{yz} bands with phonons. The width of the leading peak (*a*) is slightly (25 meV) bigger than in the case of V(100) substrate, indicating a possible difference in the lifetime of the photo hole associated with the particular *d*-QW state. However, structural effects might account for this increased value of full width at half maximum of the peak *a*, as well. Namely, it is known that defects and surface disorder contribute to the total width of the photoemission peaks.[42] Although silver monolayer films on V(100) were prepared by room-temperature deposition of silver followed by annealing at 800–900 K, silver films on Pd(111) could not have been thermally treated above 320 K without inducing strong intermixing of silver and palladium.[21] However, a more detailed temperature-dependent measurement should be done before making definite conclusions regarding the mechanisms that contribute to the width of the photoemission peaks of the *d*-derived QW states in Ag/Pd.

VI. CONCLUSIONS

We have performed experimental and computational investigation of the growth mode and the valence-band structure of ultrathin silver films deposited on Pd(111), with the

focus on the Ag 4*d*-derived quantum well states. High-resolution photoelectron spectra and *ab initio* density-functional band-structure calculations are compared for 1 and 2 ML silver films along the $\bar{\Gamma}-\bar{M}'$ high symmetry line of the surface Brillouin zone. Both, experimental and theoretical results indicate localization of the electrons of the 4*d* symmetry within the silver overlayer. The observed *d*-derived electronic states and their dispersion are explained in terms of quantum well states.

The comparison of the energy of calculated 4*d* bands in unsupported and Ag/Pd(111) films indicates rather small influence of the Pd substrate on the electronic structure of Ag-4*d*.

ACKNOWLEDGMENTS

We thank M. Kralj for the technical support for STM measurements. The financial support of the Ministry of Science, Education and Sport of the Republic of Croatia (IF group—Project No. 0035016; IRB Group—Project No. 0098001) are gratefully acknowledged.

*Corresponding author. Email address: pervan@ifs.hr

[1] T.-C. Chiang, Surf. Sci. Rep. **39**, 181 (2000).
[2] M. Milun, P. Pervan, and D. P. Woodruff, Rep. Prog. Phys. **65**, 99 (2002).
[3] A. M. Shikin, O. Rader, G. V. D. Prudnikova, V. K. Adamchuk, and W. Gudat, Phys. Rev. B **65**, 075403 (2002).
[4] J. Feydt, A. Elbe, H. Engelhard, G. Meister, and A. Goldmann, Surf. Sci. **452**, 33 (2000).
[5] A. M. Shikin, D. V. Vyalikh, G. V. Prudnikova, and V. K. Adamchuk, Surf. Sci. **487**, 135 (2001).
[6] D.-A. Luh, J. J. Paggel, T. Miller, and T.-C. Chiang, Phys. Rev. Lett. **84**, 3410 (2000).
[7] M. Kralj, P. Pervan, M. Milun, T. Valla, P. D. Johnson, and D. P. Woodruff, Phys. Rev. B **68**, 245413 (2003).
[8] E. Huger and K. Osuch, Solid State Commun. **132**, 97 (2004).
[9] J. G. Tobin, S. W. Robey, and D. A. Shirley, Phys. Rev. B **33**, 2270 (1986).
[10] J. G. Tobin, S. W. Robey, L. E. Klebanoff, and D. A. Shirley, Phys. Rev. B **35**, 9056 (1987).
[11] A. P. Shapiro, T. C. Hiseh, A. L. Wachs, T. Miller, and T.-C. Chiang, Phys. Rev. B **38**, 7394 (1988).
[12] M. Pivetta, F. Patthey, and W. D. Schneider, Surf. Sci. **532-535**, 58 (2003).
[13] U. Kürpick, G. Meister, and A. Goldmann, Surf. Sci. **328**, 58 (1995).
[14] V. Mikšić Trontl, M. Kralj, M. Milun, and P. Pervan, Surf. Sci. **551**, 125 (2004).
[15] J. M. Guglielmacci and M. Gillet, Thin Solid Films **68**, 407 (1980).
[16] B. Lang, P. Engel, and S. Tatarenko, J. Microsc. Spectrosc. Electron. **5**, 23 (1980).
[17] P. Pervan and M. Milun, Surf. Sci. **264**, 135 (1992).
[18] I. Coulthard and T. K. Sham, Phys. Rev. Lett. **77**, 4824 (1996).
[19] P. Steiner and S. Hufner, Solid State Commun. **37**, 279 (1981).
[20] B. Eisenhut, J. Stober, G. Rangelov, and Th. Fauster, Phys. Rev. B **47**, 12980 (1993).
[21] Th. Fauster, Appl. Phys. A: Solids Surf. **59**, 479 (1994).
[22] M. Williams, M. Schmidt, G. Bermes, and K. Wandelt, Rev. Sci. Instrum. **69**, 2696 (1998).
[23] M. Kralj, P. Pervan, M. Milun, P. Lazić, Ž. Crljen, R. Brako, J. Schneider, A. Rosenhahn, and K. Wandelt, Phys. Rev. B **68**, 195402 (2003).
[24] G. Fuster, J. M. Tyler, N. E. Brener, J. Callaway, and D. Bagayoko, Phys. Rev. B **42**, 7322 (2003).
[25] J.-S. Kang, D. W. Hwang, C. G. Olson, S. J. Youn, K.-C. Kang, and B. I. Min, Phys. Rev. B **56**, 10605 (1997).
[26] B. Frick and K. Jacobi, Phys. Rev. B **37**, 4408 (1988).
[27] L.-G. Petersson, R. Malander, D. P. Spears, and S. B. Hagström, Phys. Rev. B **14**, 4177 (1976).
[28] A. Elbe, G. Meister, and A. Goldmann, Surf. Sci. **397**, 346 (1998).
[29] G. Rangelov, Th. Fauster, U. Strüber and J. Küppers, Surf. Sci. **331-333**, 948 (1995).
[30] R. Fischer, S. Schuppler, N. Fischer, Th. Fauster, and W. Steinmmann, Phys. Rev. Lett. **70**, 654 (1993).
[31] D.-A. Luh, T. Miller, J. J. Paggel, M. Y. Chou, and T.-C. Chiang, Science **292**, 1131 (2001).
[32] In some cases, a lack of hybridization gaps results in formation of QW resonances that can be clearly observed in photoemission spectra (e.g., Cu/Co(100), see, e.g., C. Carbone, E. Vescovo, R. Kläsges, D. D. Sarma, and W. Eberhardt, Solid State Commun. **100**, 749 (1996).
[33] J. Hermanson, Solid State Commun. **22**, 9 (1977).
[34] P. S. Wehner, R. S. Williams, S. D. Kevan, D. Denley, and D. A. Shirley, Phys. Rev. B **19**, 6164 (1979).
[35] V. M. Trontl, I. Pletikosić, M. Milun, and P. Pervan (unpublished).
[36] E. D. Hansen, T. Miller, and T.-C. Chiang, J. Phys.: Condens. Matter **9**, L435 (1997).
[37] A. Mugarza, J. E. Ortega, A. Mascaraque, E. G. Michel, K. N. Altmann, and F. J. Himpsel, Phys. Rev. B **62**, 12 672 (2000).
[38] T. Miller, J. J. Paggel, D.-A. Luh, and T.-C. Chiang, J. Electron Spectrosc. Relat. Phenom. **114-116**, 513 (2001).
[39] M. Milun, P. Pervan, B. Gumhalter, and D. P. Woodruff, Phys. Rev. B **59**, 5170 (1999).
[40] V. Mikšić Trontl, Ph.D. thesis, Faculty of Natural Sciences, University of Zagreb, November 2005.
[41] J. J. Paggel, T. Miller, and T.-C. Chiang, Science **283**, 1709 (1999).
[42] F. Theilmann, R. Matzdorf, and A. Goldman, Surf. Sci. **420**, 33 (1999).